Geomechanics and Engineering, *Vol. 34, No. 5 (2023) 577-595*
https://doi.org/10.12989/gae.2023.34.5.577

Discrete element numerical simulation of dynamic strength characteristics of expanded polystyrene particles in lightweight soil

Wei Zhou[1], Tian-shun Hou*[1], Yan Yang[1], Yu-xin Niu[1], Ya-sheng Luo[1] and Cheng Yang[2]

[1]*College of Water Resources and Architectural Engineering, Northwest A&F University, Yangling 712100, Shaanxi, China*
[2]*Hanjiang to Weihe River Valley Water Diversion Project Construction Co., Ltd., Shaanxi Province, Xi'an 710011, Shaanxi, China*

(*Received September 23, 2022, Revised July 14, 2023, Accepted July 20, 2023*)

Abstract. A dynamic triaxial discrete element numerical model of lightweight soil was established using the discrete element method to study the microscopic mechanism of expanded polystyrene (EPS) particles in the soil under cyclic loading. The microscopic parameters of the discrete element model of the lightweight soil were calibrated depending on the dynamic triaxial test hysteresis curves. Based on the calibration results, the effects of the EPS particles volume ratio and amplitude on the contact force, displacement field, and velocity field of the lightweight soil under different accumulated strains were studied. The results showed that the hysteresis curves of lightweight soil exhibit nonlinearity, hysteresis, and strain accumulation. The strain accumulated in remolded soil is mainly tensile strain, and that in lightweight soil is mainly compressive strain. As the volume ratio of EPS particles increased, the contact force first increased and then decreased, and the displacement and velocity of the particles increased accordingly. With an increase in amplitude, the dynamic stress of the particle system increased, and the accumulation rate of the dynamic strain of the samples also increased. At 5% compressive strain, the contact force of the particles changed significantly and the number of particles deflected in the direction of velocity also increased considerably. These results indicated that the cemented structure of the lightweight soil began to fail at a compressive strain of 5%. Thus, a compressive strain of 5% is more reasonable than the dynamic strength failure standard of lightweight soil.

Keywords: cyclic load; discrete element method; dynamic triaxial test; lightweight soil; microscopic mechanism

1. Introduction

Loess is widely distributed in China. Loess collapsibility garnered attention during highway construction in loess areas. Several measures can be implemented to deal with loess collapsibility, such as dynamic compaction, chemical reinforcement, and compaction piles. However, in the long term, subgrade settlement caused by collapsibility is inevitable. To completely solve this problem, expanded polystyrene (EPS) particles in lightweight soil with the characteristics of low weight and high strength have been studied (Hou and Xu 2009, Hou and Xu 2010, Hou *et al.* 2011). Lightweight soil with EPS particles is a new type of geotechnical material consisting of raw soil, cement, EPS particles, and water. A curing agent can enhance the strength of mixed soil, and EPS particles can significantly reduce the density and weight of mixed soil (Hou and Xu, 2011, Hou 2012).

In practical engineering, subgrade filling primarily bears the dynamic load. The dynamic characteristics of EPS particles in lightweight soil were studied using dynamic triaxial tests. The results showed that the accumulative plastic deformation of lightweight soil was the result of strength instability under cyclic loading. The confining pressure, cement content, and EPS particle content influence the dynamic strength of lightweight soil (Zhou *et al.* 2008, Dong *et al.* 2019). Dynamic triaxial tests can reveal only the macroscopic deformation of soil under cyclic loading and not the law governing the variation in the mechanical response of the internal particles under different cumulative strains of the soil. The research objects in the field of geotechnical engineering are discontinuous particle aggregates, which can be regarded as particles with the same mechanical behavior. These particles exhibit complex interactions. The particle flow program based on the discrete element theory provides a new way to reveal the microscopic mechanisms of soil (Cundall and Strack 1979).

Large-scale triaxial tests and discrete element numerical simulations of cemented soil–rock mixtures were conducted, and the meso-failure mechanism was analyzed (Jin *et al.* 2017). In the modeling of the soil–rock mixture, the three-dimensional discrete element modeling technology of irregular rock blocks and soil–rock mixtures was applied. The results showed that microcracks begin at the soil–rock interface, diffuse in the soil, bypass the rock blocks, and finally form multiple flexural failure zones in the entire sample. The effects of cementation on the shear dilatancy and strength of cemented sand were studied using triaxial tests and discrete element numerical simulations (Wang and Leung 2008). When the strain level was lower, a mesh force chain was formed in the soil, hindering the shear dilatancy of the cemented sand. When the soil reached the yield state, the shear dilatancy of the soil increased its strength. With an increase in cement content, the shear dilatancy rate of the soil increased. The complete

*Corresponding author, Associate Professor
E-mail: houtianshunyx@sina.com

ISSN: 2005-307X (Print), 2092-6219 (Online)

Table 1 Basic physical parameters of the soil

Natural moisture content /w (%)	Specific gravity /G_s	Natural density /ρ (g/cm^3)	Plastic limit /w_p (%)	Liquid limit /w_L (%)	Plasticity index /I_P	Liquid index /I_L	Void ratio /e
19.8	2.72	1.75	20.8	33.9	13.1	−0.07	0.86

cementation contact model was introduced into the discrete element program, and the influences of the cementation strength between particles and the cyclic stress ratio on the sample were studied (Zhang *et al.* 2021). For samples with a certain bond strength, the bond failure increased with an increase in the cyclic stress ratio, and the distribution of bond points existed in the tangential and normal directions.

When the parallel-bonding model was used in the cementing system, quantifying the models according to different cement contents was difficult. Therefore, a contact model using a particle flow program was established to simulate the interlocking effect of cemented blocks (Dong and Fatahi 2020). This model could quantify cemented sand with different cement contents. The stress–strain relationship and strength characteristics of the cemented sand were studied using a cementation model. The results showed that cementation can improve the strength of soil but has little effect on the internal friction angle of the soil. Under a high confining pressure, owing to the degradation of cementation, the failure envelope of the cemented sand gradually merged with the critical state line. The failure mode of cemented sand was primarily controlled by the shear force at the contact interface rather than the tensile strength. The discrete element model of the structural soil was established using the soft–hard composite cementation contact model. The relationship between the cementation damage process and macroscopic mechanical behavior was studied (Li *et al.* 2020). True triaxial tests were simulated to explore the influence of the stress path on the cementation damage of the structural soil. To quantitatively express the degree of cementation damage in cemented soil, the "cementation damage" parameter was defined. Cementation damage was found to be related to the stress path, and the relationship between the parameter denoting cementation damage and the stress path can be expressed by an exponential function.

Lightweight soil is a type of mixed-medium system that depends on cementation strength to bond the particles together. The particle behavior is similar to that of a particle system with cementation strength, and the influence of the microscopic parameters is nearly identical. A numerical model of lightweight soil was established for dynamic triaxial tests using the PFC3D discrete element software for the first time. The feasibility of the numerical model of lightweight soil was demonstrated by comparing the hysteresis curves of dynamic triaxial tests and numerical simulations, and the basic relationship between microscopic parameters and macroscopic mechanical response was studied (Lan *et al.* 2020). The internal structure of EPS particles in lightweight soil is complex, and the motion law of the internal particles at different strain accumulation levels under cyclic loading is unknown. The variation law of the particle contact force, displacement field, and velocity field under different strains can be revealed by employing the particle flow program, which connects the microscopic mechanism with the macroscopic mechanical response and provides a reference at the meso-scale to reveal the dynamic strength characteristics of lightweight soil.

2. Dynamic triaxial tests of lightweight soil

2.1 Test materials and sample preparation

The raw soil used in the tests was Q_3 loess from Yangling, Shaanxi Province, China. The soil was yellowish brown with low-liquid-limit silty clay. The basic physical indices of the samples are listed in Table 1. Standard light compaction tests were conducted according to the *Standard for Geotechnical Testing Method* (GB/T50123-2019). The measured optimal moisture content of the raw soil was 21.6% and the maximum dry density was 1.701 g/cm^3. The EPS particle size was 1–3 mm, bulk density was 0.025 g/cm^3, and pure particle density was 0.0312 g/cm^3. The curing agent was P32.5 ordinary Portland cement, and ordinary tap water was used.

To prepare lightweight soil samples, the raw soil was dried, crushed, and then sieved through a 2-mm sieve. First, cement and water were added to the raw soil to form a cement slurry. Then, EPS particles were added and stirred to form a uniform mixture. The mixture was poured into a three-lobe mold having a height of 8 cm and a diameter of 3.91 cm by pouring method. To facilitate demolding, a preservative film layer was placed on the inner surface of the three-lobe mold before pouring. The finished samples were then placed in a curing box (humidity ≥ 95%, temperature = 20℃) for maintenance. After 3 d of maintenance, the samples were demolded and maintained until the 28th day.

The remolded soil samples were prepared using the compaction method. The hammer weight of the small compaction instrument was 305 g, and the falling distance was 24.8 cm. The samples were then compacted into three layers. Based on the compaction work, the number of hits per layer was set as 23. The samples were saturated before the tests, placed under vacuum for 2 h, and then saturated with water for 24 h.

2.2 Test scheme

The mixture ratio of lightweight soil was based on the mass of dry soil. The moisture content was $w = m_w/m_s \times 100\%$, where m_w is the mass of water. The cement content was $a_c = m_c/m_s \times 100\%$, where m_c is the mass of the cement. The volume ratio of EPS particles was $b_e = v_e/v \times 100\%$,

Table 2 Dynamic triaxial test scheme

Influence factor	Scheme 1	Scheme 2	Scheme 3
EPS particle volume ratio /b_e (%)	20, 40, 60	40	0
Cement content / a_c (%)	15	10, 15, 20	0
Moisture content / w (%)	50	50	w_{op} = 21.6%
Age /T (d)	28	28	0
Confining pressure /σ_3 (kPa)	50, 100, 150, 200	50, 100, 150, 200	50, 100, 150, 200
Frequency /f (Hz)	1	1	1

where v_e is the EPS particles volume and v is the sample volume. The optimal moisture content was used to prepare remolded soil samples.

The test instrument was an SDT-20 microcomputer controlled electro-hydraulic servo dynamic triaxial test machine manufactured by Xi'an Lichuang. The test scheme is presented in Table 2. The tests should end when the strain of the samples reach 10% within 100 vibration cycles. To meet the requirements of the tests, the appropriate amplitude of each sample was determined by conducting multiple tests. We found that the same lightweight soil samples with higher strength had difficulty reaching 10% strain in the tests; therefore, 5% strain was selected as the end standard for these samples.

2.3 Test result analysis

Fig. 1 shows the following: (1) the hysteresis curves of remolded soil move left along the strain axis, and the strain accumulated is mainly tensile strain. When the confining pressure is constant, the area of the hysteresis loop changes from small to large with the increase in vibration cycle numbers. The hysteresis loop exhibits a trend from dense to sparse. (2) The hysteresis curves of the lightweight soil move right along the strain axis, and the strain accumulated is mainly compressive strain. When the confining pressure is constant, the area under the hysteresis loop changes from small to large with an increase in the dynamic strain. When the confining pressures are 150 kPa and 200 kPa, the area of the hysteresis curves of lightweight soil samples with 15% cement content and 60% EPS particle volume ratio shows the opposite trend of first increasing and then decreasing as the strain increases. (3) With the decrease in EPS particle volume ratio and increase in cement content, the stiffness of the sample increases, causing the deformation of the rubber membrane of the sample to increase during vibration. The rubber membrane of the sample breaks before reaching a strain of 10%. Therefore, the samples with an EPS particle volume ratio of 20% cannot reach 10% strain, and the samples with a cement content of 20% cannot reach 10% strain at a confining pressure of 200 kPa. The hysteresis curve vibration of these samples ends when the compressive strain reaches 5%. (4) The hysteresis curves of lightweight soil have a small area from the maximum tensile strain to the zero point of strain, almost zero, so that it almost overlapps into a straight line. The maximum tensile strain reaches 25%. (5) The hysteresis curves of the lightweight soil and remolded soil exhibit strain accumulation. Except for few samples, the hysteresis loops are dense in the early stages of vibration, and the structure of the samples is not destroyed. The elastic deformation of the samples under cyclic loading is greater than that under plastic loading. With an increase in vibration time, the structure of the sample is destroyed, the elastic deformation disappears gradually, and the plastic deformation increases rapidly. (6) The amplitudes of the tension and compression half-cycles of the hysteresis curves for lightweight soil are not equal, and the amplitude of the tension half-cycle is less than that of the compression half-cycle. The strain accumulated is mainly compressive strain. The amplitudes of the tension and compression half-cycles of the remolded soil hysteresis curves are approximately equal, and the strain accumulated is mainly tensile strain.

The hysteresis curve refers to the relationship curve between the dynamic stress and dynamic strain of the soil during vibration. Hysteresis curves reflect the hysteretic characteristics of dynamic stress and strain changes in different phases of the soil under cyclic loading, indicating that the soil has viscous characteristics. Under the continuous action of the same dynamic stress, the centers of the hysteresis curves move continuously on the dynamic strain axis, and plastic deformation occurs in the sample.

The moving distance of the hysteresis curves is not equal for each vibration, indicating that the samples have a certain elastic deformation. The hysteresis curves show the complex viscoelastic–plastic properties of the soil. Under cyclic loading, the hysteresis curves of remolded soil or lightweight soil exhibit three typical characteristics: nonlinearity, hysteresis, and strain accumulation. Theoretically, the hysteresis curve is closed with equal tensile and compressive amplitudes. The tensile and compressive amplitudes of the hysteresis curves of the remolded soil were equal, but those tensile and compressive amplitudes of the lightweight soil were not equal. During the tests, we found that the rubber membrane of the lightweight soil sample separated from the sample under tensile stress loading. The tensile stress was not loaded onto the sample but was added to the rubber membrane. With an increasing vibration time, the rubber membrane underwent elastic deformation under tensile stress. The elastic deformation did not accumulate during the loading and unloading process of the tensile stress. Therefore, the tensile strain of the hysteresis curves of the lightweight soil was larger, and the amplitudes of the tensile and compressive half-cycles were not equal.

3. Discrete element numerical simulation of lightweight soil

3.1 Establishment of particle system

Three types of particles are present in lightweight soil with EPS particles: soil, cement, and EPS particles. Compared with the other two types of particles, the size of cement particles is very small. The products of hydrolysis and hydration reactions in soil are extremely complex.

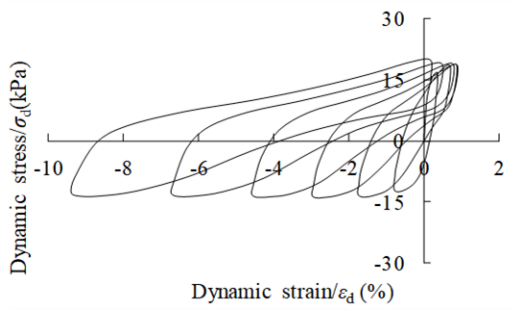

(1) Confining pressure of 50 kPa

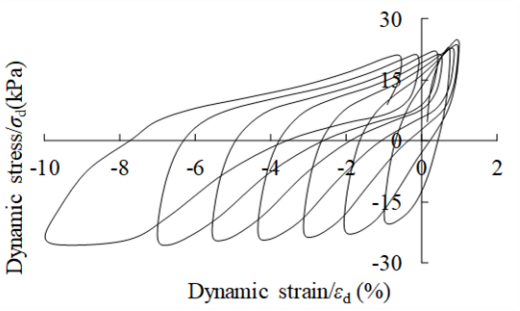

(2) Confining pressure of 100 kPa

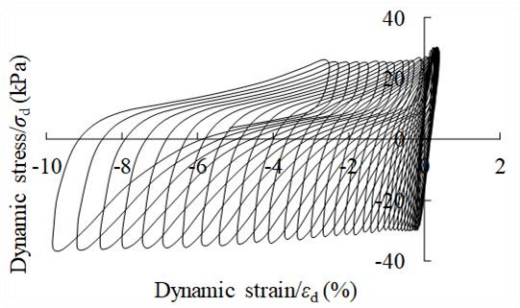

(3) Confining pressure of 150 kPa

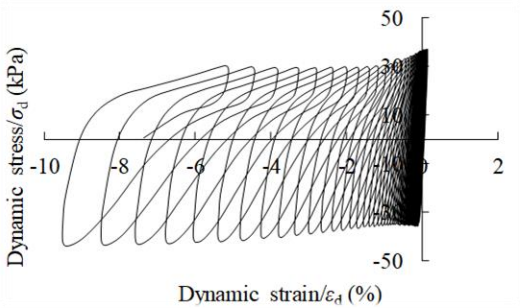

(4) Confining pressure of 200 kPa

(a) Remolded soil

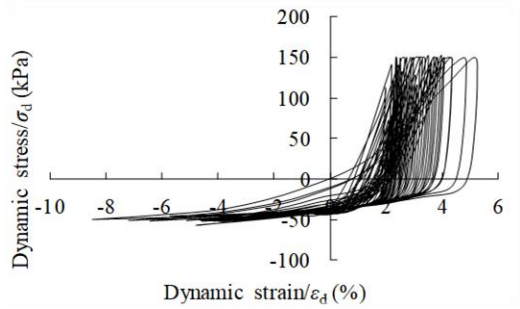

(1) Confining pressure of 50 kPa

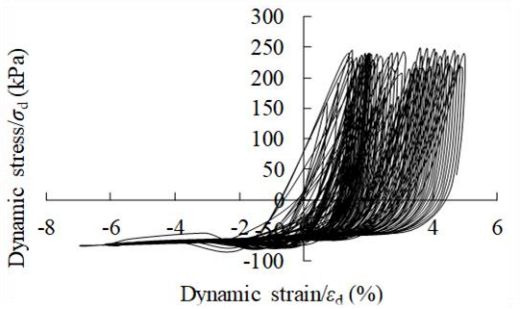

(2) Confining pressure of 100 kPa

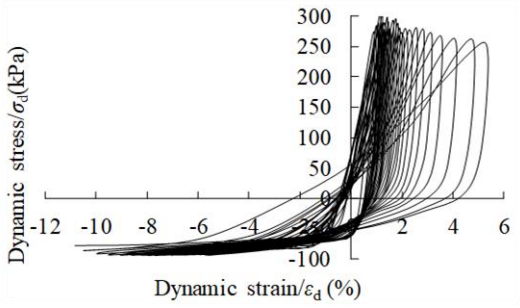

(3) Confining pressure of 150 kPa

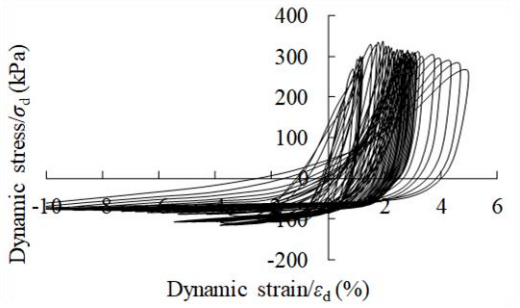

(4) Confining pressure of 200 kPa

(b) a_c = 15%, b_e = 20%

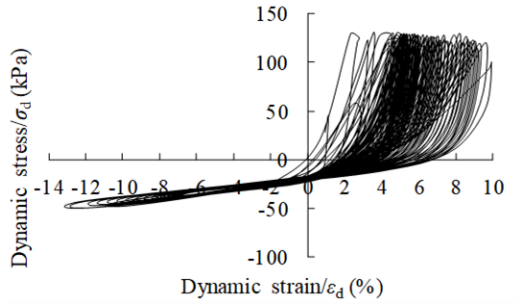

(1) Confining pressure of 50 kPa

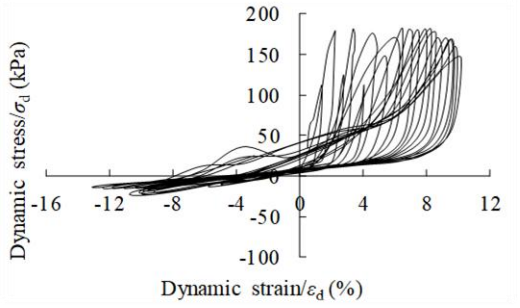

(2) Confining pressure of 100 kPa

Fig. 1 Hysteresis curves from dynamic triaxial tests

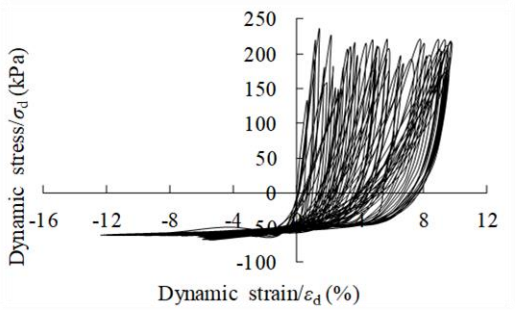

(3) Confining pressure of 150 kPa

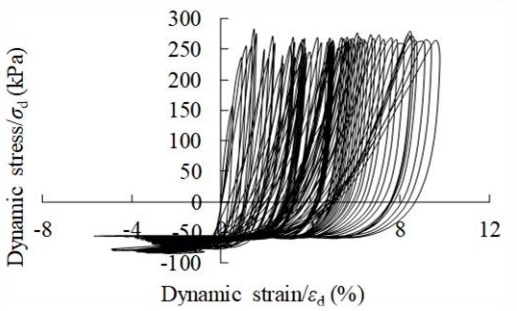

(4) Confining pressure of 200 kPa

(c) a_c = 15%, b_e = 40%

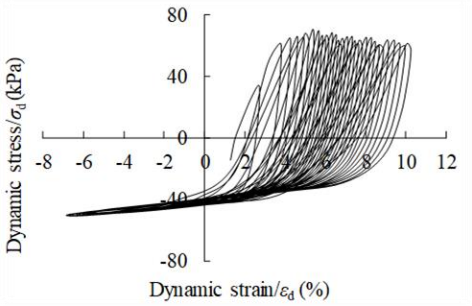

(1) Confining pressure of 50 kPa

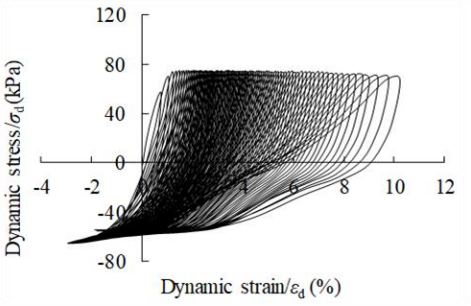

(2) Confining pressure of 100 kPa

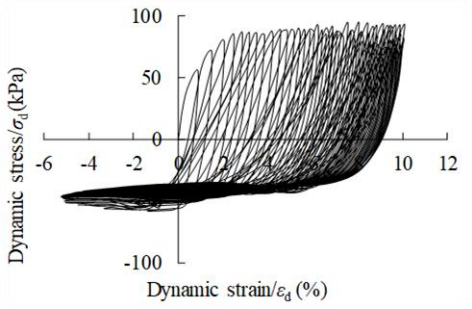

(3) Confining pressure of 150 kPa

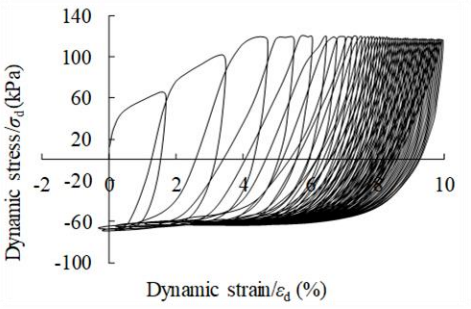

(4) Confining pressure of 200 kPa

(d) a_c = 15%, b_e = 60%

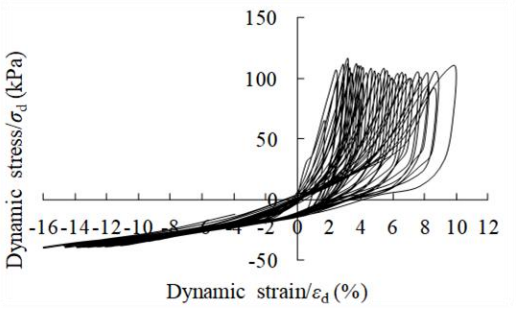

(1) Confining pressure of 50 kPa

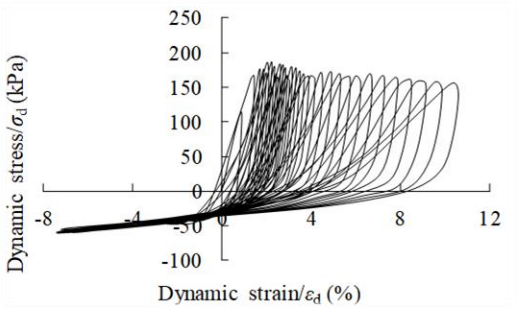

(2) Confining pressure of 100 kPa

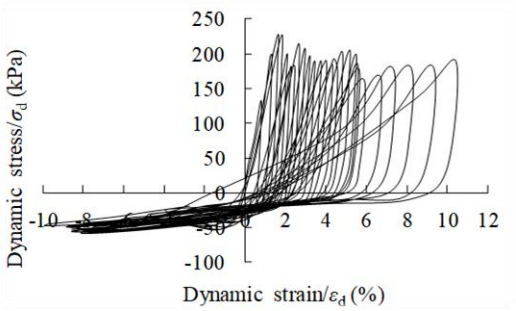

(3) Confining pressure of 150 kPa

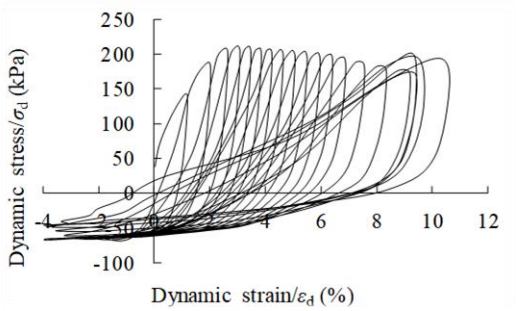

(4) Confining pressure of 200 kPa

(e) a_c = 10%, b_e = 40%

Fig. 1 Continued-

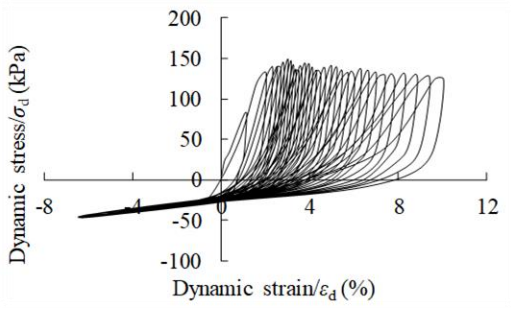

(1) Confining pressure of 50 kPa

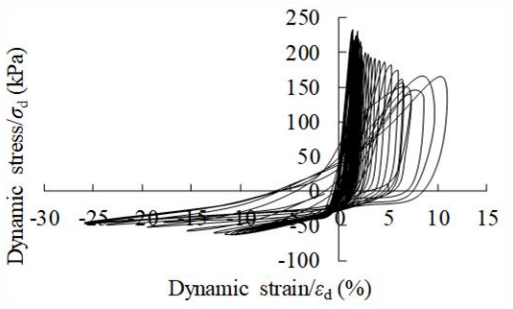

(2) Confining pressure of 100 kPa

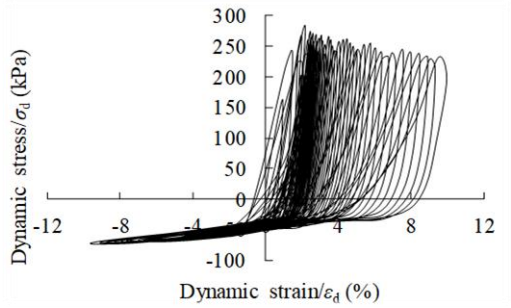

(3) Confining pressure of 150 kPa

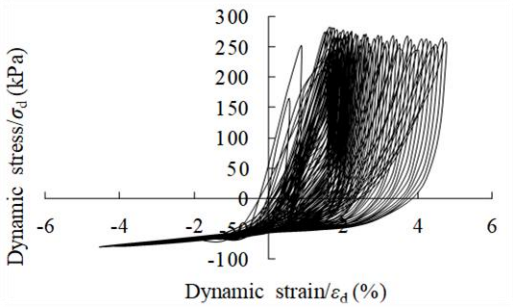

(4) Confining pressure of 200 kPa

(f) a_c = 20%, b_e = 40%

Fig. 1 Continued-

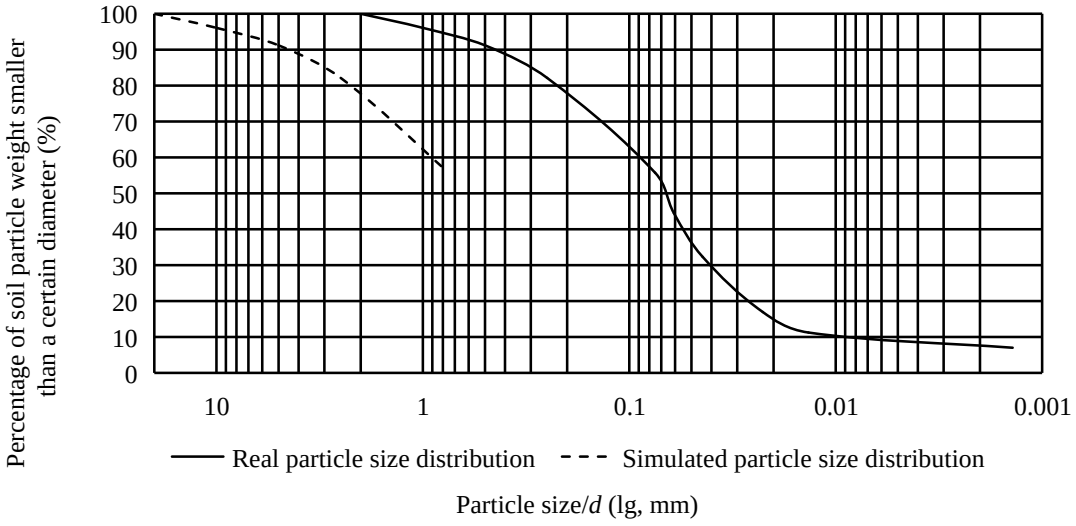

Fig. 2 Gradation cumulative curve of soil particles in the numerical model of lightweight soil

Therefore, the cement particles are regarded as the bond strength in the model. In the discrete element model of lightweight soil, only soil particles and EPS particles are present and grouped according to different stiffnesses. Soil particles are generated as per gradation (Anandarajah 1994, Batiste *et al*. 2004, Xu *et al*. 2016). In the discrete element simulation of lightweight soil, the radius expansion method is used to amplify the particle size distribution by a certain factor, and the amplified particle can be considered to be representative of a group of particles with similar mechanical properties. To improve calculation efficiency, the size of the coarse particle group of soil particles is enlarged by 10 times. Because of the viscosity of the fine particle group, this group is considered as a type of bonding, and the generated soil particle system only considers the coarse particle group. The gradation cumulative curve of soil particles in the numerical model of lightweight soil is shown in Fig. 2.

When the particles are generated according to the gradation, if the size of the EPS particles is increased by 10 times, the EPS particles will overflow the calculation boundary during sample generation. To achieve the set volume ratio, the EPS particle size was modeled to be 1–3 mm. The particle generation process is illustrated in Fig. 3. Three types of lightweight soil samples were generated based on the EPS particle volume ratios of 20%, 40%, and

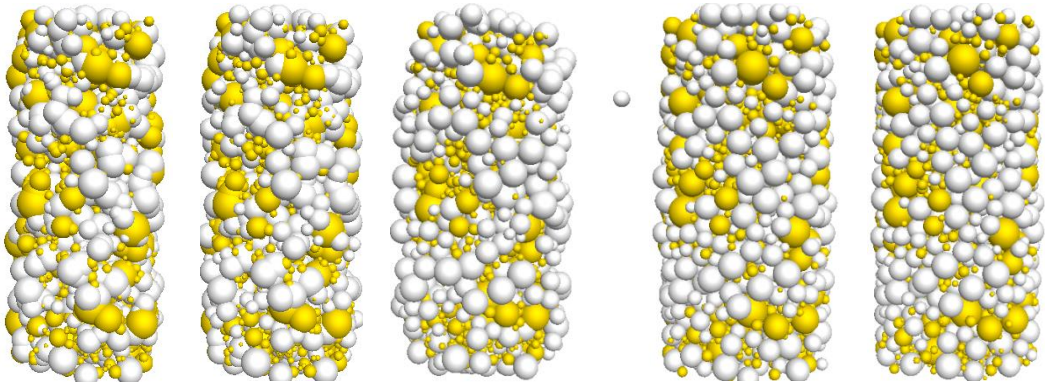

Fig. 3 Generation process of dynamic triaxial test numerical sample for lightweight soil

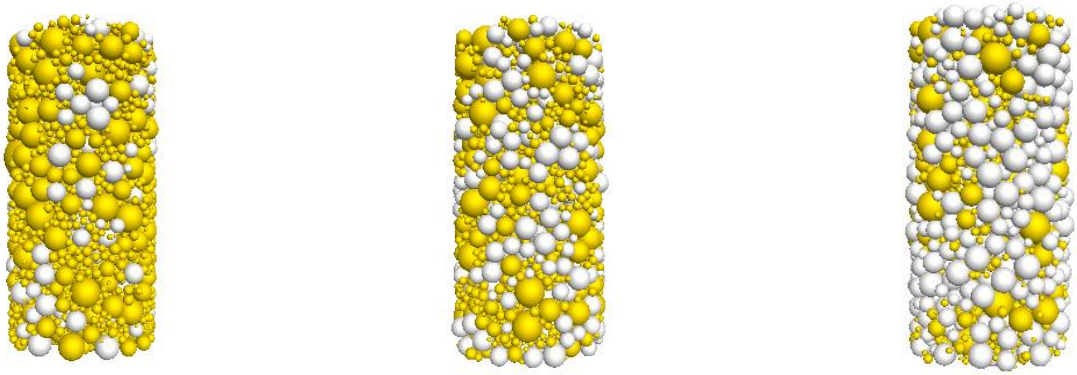

(a) b_e = 20% (b) b_e = 40% (c) b_e = 60%

Fig. 4 Numerical sample of lightweight soil

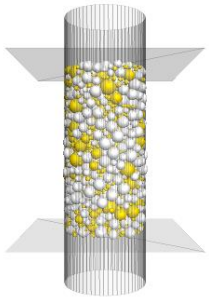

Fig. 5 Dynamic triaxial loading boundary of lightweight soil

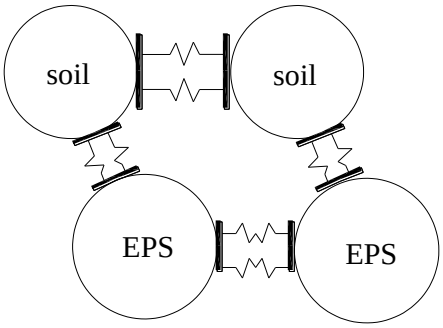

Fig. 6 Contact-bonding model of lightweight soil

60%. This is shown in Fig. 4. The yellow and white spheres represent soil and EPS particles, respectively.

3.2 Loading boundary establishment

The wall was the boundary of servo control in the discrete element program, and it was set as rigid in the dynamic triaxial tests. The walls were divided into two types. The first was the confining pressure servo boundary, which was simulated by using a cylindrical wall. The stiffness was set to be 1/10 of the soil particle stiffness. The second was the loading boundary of the cyclic load simulated by using a rigid plane wall. The established dynamic triaxial loading boundary of lightweight soil is shown in Fig. 5.

3.3 Contact model and microscopic parameter calibration

In the discrete element numerical simulation of general soil, the contact bond model is typically adopted without considering the transfer effect of torque in the bonds (Bono *et al.* 2012, Wu and Xu 2016, Lv *et al.* 2019; Yang *et al.* 2020). Compared with soil particles and EPS particles, the size of cement particles is very small. The reactants produced by the cement hydration reaction are wrapped around the surface of the soil particles. Simultaneously, owing to the smaller stiffness of the EPS particles, a larger deformation occurs in the process of sample preparation and shear. Therefore, the bonding among the particles is not a point-to-point contact. Torque transfer occurs among the

Table 3 Parallel-bonding contact parameters of discrete element numerical model for lightweight soil

Objects	Stiffness parameters		Strength parameters			
	Deformation modulus /pb_deform (Pa)	Stiffness ratio	Tangential bond strength /pb_ten (Pa)	Normal bond strength /pb_con (Pa)	Internal friction angle /pb_fa (°)	Bonding radius /pb_rad
Soil–Soil	1×10^8	2	4×10^8	4×10^8	20	1.0
Soil–EPS	—	—	1×10^8	1×10^8	15	1.0
EPS–EPS	1×10^7	1	3×10^7	3×10^7	10	1.0

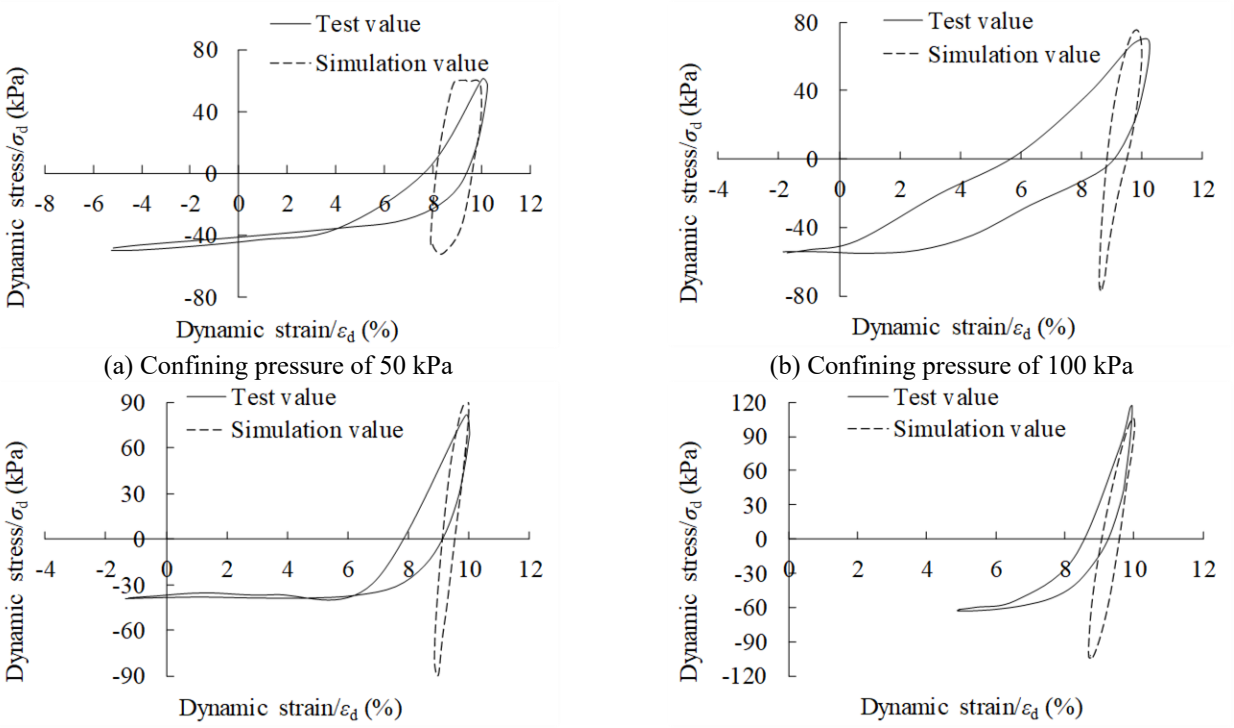

(a) Confining pressure of 50 kPa

(b) Confining pressure of 100 kPa

(c) Confining pressure of 150 kPa

(d) Confining pressure of 200 kPa

Fig. 7 Comparison of test and simulation hysteresis curves of dynamic triaxial tests for lightweight soil (a_c = 15%, b_e = 60%)

particles, and the bonding strength of the samples is very high. Therefore, the parallel-bonding model was used as the contact model for the lightweight soil samples. A contact diagram of the lightweight soil particles is shown in Fig. 6.

The hysteresis curve, which is the constitutive relationship curve of the soil under cyclic loading, best reflects the dynamic characteristics of the soil. Therefore, the meso-parameters of the dynamic triaxial discrete element simulation of lightweight soil were calibrated using the test hysteresis curves. The sample with b_e = 60% was subjected to constant-amplitude cyclic loading, and the parameters were calibrated using the last-lever hysteresis curve. The hysteresis curves of the experiment were compared with those of the simulation to continuously adjust the microscopic parameters so that the shape of the experimental hysteresis curves was roughly similar to that of the simulation curves. The results are shown in Fig. 7.

The microscopic parameters mainly included attribute and contact parameters. The attribute parameters were found in previous studies (Lan *et al*. 2020). The contact parameters were adjusted through calibration. The parameters, calibrated according to the results shown in Fig. 7, are listed in Table 3.

4. Variation in microscopic mechanical characteristics of lightweight soil under different cumulative compressive strains

4.1 Influence of EPS particle volume ratio on microscopic mechanical characteristics of lightweight soil

Under the premise of a constant confining pressure of 100 kPa and cement content of 15%, samples with EPS particle volume ratios of 20%, 40%, and 60% were subjected to cyclic loading. To study the influence of the EPS particle volume ratio on the particle motion in different strain development processes, the amplitude and confining pressure must be fixed. In the simulation process, when the

Table 4 Dynamic triaxial test numerical simulation scheme of lightweight soil with different EPS particle volume ratios

EPS particle volume ratio /b_e (%)	Cement content /a_c (%)	Confining pressure /σ_3 (kPa)	Amplitude /σ_d (kPa)
20, 40, 60	15	100	180

amplitude was extremely small, the strain of the sample with an EPS particle volume ratio of 20% remained unchanged after accumulating to a fixed value, which could not reach 10%. Therefore, the simulated amplitude was 180 kPa. In the simulation process, the loading stop standard was the first time that the compressive strain reached a set value in the loading stage. The simulation scheme is presented in Table 4.

(1) Contact force

Fig. 8 reveals the following: (1) the force chain between soil particles is the thickest, indicating that the lightweight soil is mainly borne by the skeleton formed by the bond between soil particles under load. (2) When the EPS particle volume ratio is constant, the contact force increases with an increase in compressive strain. (3) When the compressive strain is constant, with an increase in the EPS particle volume ratio, the contact force first increases and then decreasesd. (4) The contact force chain between EPS particles is the smallest, and with an increase in the EPS particle volume ratio, the force chain among EPS particles increases, filling within the force chain skeleton composed of soil particles. (5) With the increase in compressive strain in the soil, the contact force chain between the EPS particles breaks. When the EPS particle volume ratios are 20% and 40%, the contact force among the soil particles decrease with an increase in the compressive strain in the soil. However, for the lightweight soil sample with an EPS particle volume ratio of 60%, the contact force between the soil particles changes slightly with the increase in the compressive strain in the soil. This is because the sample with a lower EPS particle content has obvious brittleness. When the compressive strain in the soil is small, penetrating cracks are formed, and some particles lose their constraints.

The contact force between the particles changes significantly at a strain of 5%. The hysteresis curves of the lightweight soil in Fig. 1 begin to change from dense to sparse at 5% strain, indicating that the structure is destroyed and the deformation accumulation rate is accelerated. Corresponding to the microscopic change in the contact force, the contact force between the particles decreases and the particles undergo displacement.

(2) Displacement field

Fig. 9 shows the following: (1) the particle displacement value of the lightweight soil sample decreases from the ends to the center of the sample, and the particle displacement value at both ends of the sample is the largest. (2) When the EPS particle volume ratio is constant, the displacement of particles increases with an increase in strain, but the increase rates are small. (3) The displacement of the particles is mainly along the vertical direction towards the center of the sample. When the compressive strain is 2%, a penetrating crack parallel to the top and bottom surfaces appears in the upper-left part of the sample with a 20% EPS particle volume ratio, and no obvious shear band appears in the other samples.

The displacement field reveals that the particle displacement of lightweight soil does not change significantly with the increase in compressive strain under cyclic loading because a strong bond exists between the lightweight soil particles. The decrease in the EPS particle volume ratio increases the brittleness of the samples, resulting in cracks in the sample at 2% strain and indicating the brittleness of the soil. Failure of the samples occurs earlier under cyclic loading, indicating that the strength of the samples decreases under cyclic loading. For samples with lower EPS particle volume ratios, the failure strain in the soil should be smaller.

(3) Velocity field

Fig. 10 displays the following: (1) under the same compressive strain, the particle velocity increases with an increase in the EPS particle volume ratio. (2) Under the same EPS particle volume ratio, the particle velocity increases with an increase in the compressive strain. (3) In the early stage of the vibration, the distribution of the particle velocity direction is not obvious. With the increase in compressive strain, the particle velocity direction exhibits a directional arrangement and the number of particles with velocity direction deflection increases significantly when the compressive strain is 5%. The particle velocity at both ends of the sample is along the radial direction from the center. With an increase in the EPS particle volume ratio, the particle velocity at the middle changed along the vertical direction towards the center of the sample to the radial from the center. Moreover, the particle velocities at both ends are greater than that at the middle.

An increase in the EPS particle volume ratio indicates a decrease in the number of soil particles in the sample. For lightweight soil samples, the strength of the bond between the soil particles is the basis of the strength of the lightweight soil. The larger the EPS particle volume ratio, the lower the strength of the soil, the smaller the constraint between particles, and more easily the bonding fails. Under the same dynamic stress, the velocity of the particles is also larger.

EPS particles are mainly used as weight-reducing materials in lightweight soils. The cementation between the EPS particles and soil particles is weak, and it is easily destroyed under cyclic loading. The different EPS particle volume ratios of lightweight soil resulted in different overall structural strengths of the samples. The larger the EPS particle volume ratio, the lower the structural strength of the samples and the weaker the contact force between the particles. In the sample with an EPS particle volume ratio of 20%, a penetrating crack appeared at the upper end of the sample when the strain reached 2%. This indicated that the smaller the EPS particle volume ratio, the more evident the brittle failure characteristics of the sample. In engineering applications, enhancing the strength by increasing the cement content or reducing the EPS particle volume ratio is

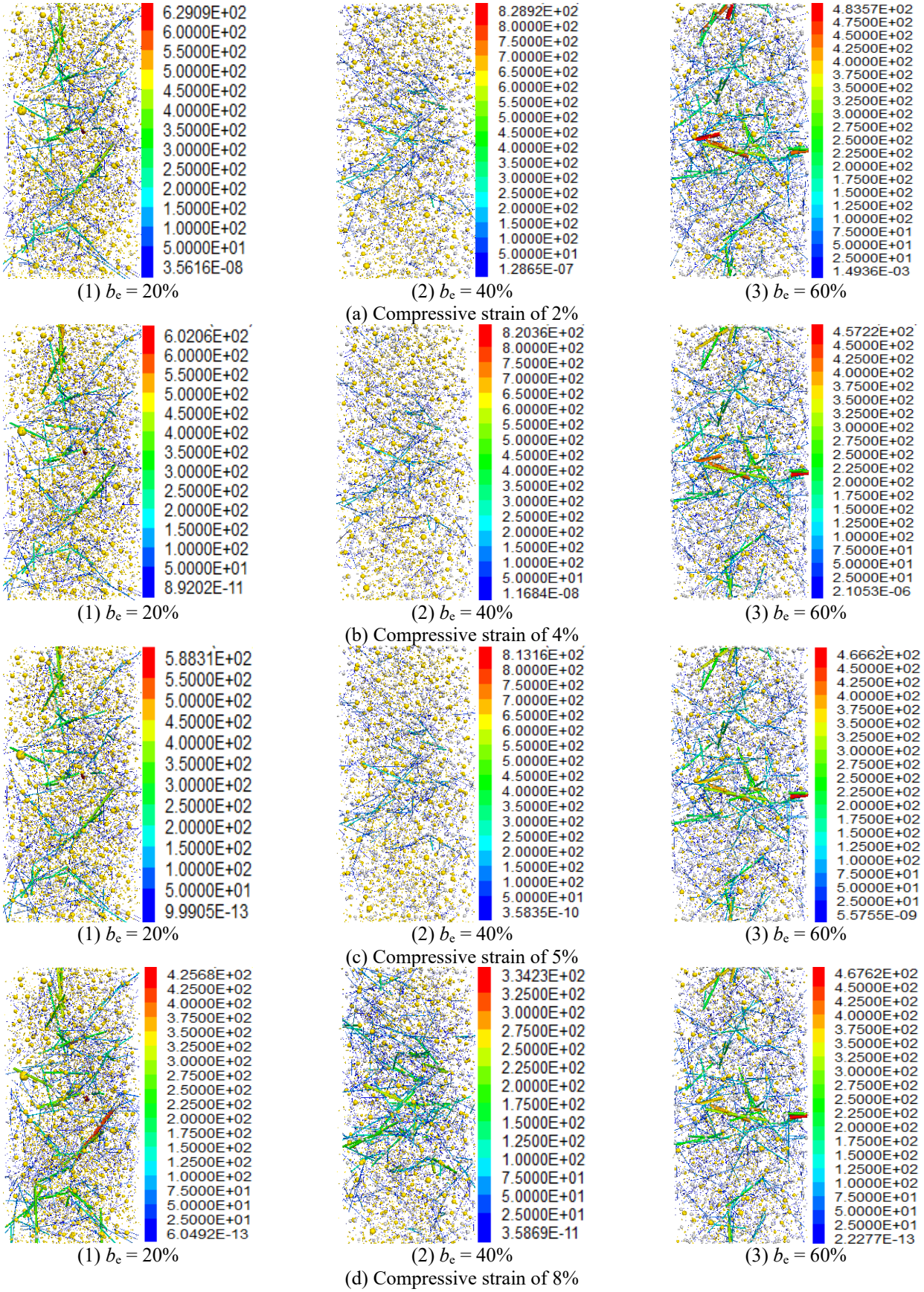

(1) b_e = 20% (2) b_e = 40% (3) b_e = 60%

(a) Compressive strain of 2%

(1) b_e = 20% (2) b_e = 40% (3) b_e = 60%

(b) Compressive strain of 4%

(1) b_e = 20% (2) b_e = 40% (3) b_e = 60%

(c) Compressive strain of 5%

(1) b_e = 20% (2) b_e = 40% (3) b_e = 60%

(d) Compressive strain of 8%

Fig. 8 Change law of contact force of lightweight soil with different EPS particle volume ratios (σ_3 = 100 kPa, σ_d = 180 kPa, unit of contact force: N)

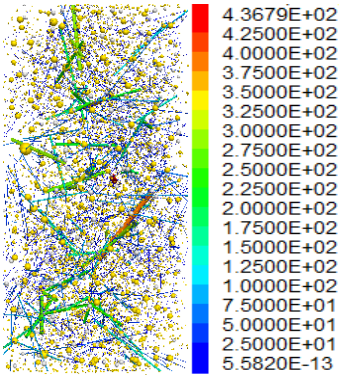

(1) b_e = 20%

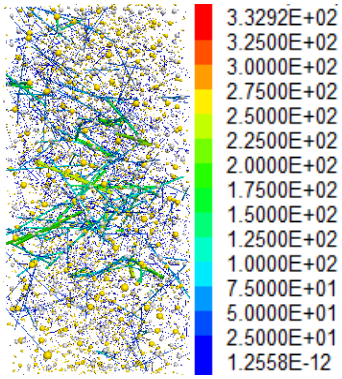

(2) b_e = 40%

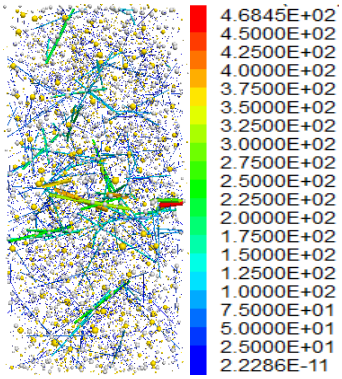

(3) b_e = 60%

(e) Compressive strain of 10%

Fig. 8 Continued-

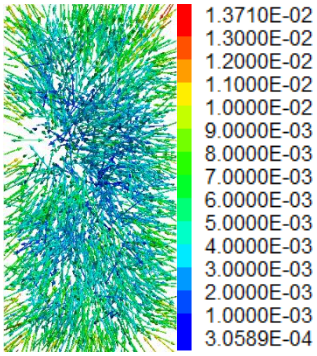

(1) b_e = 20%

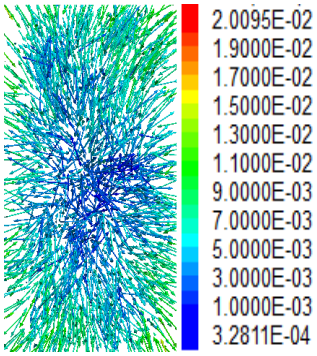

(2) b_e = 40%

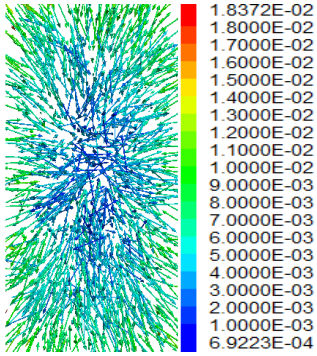

(3) b_e = 60%

(a) Compressive strain of 2%

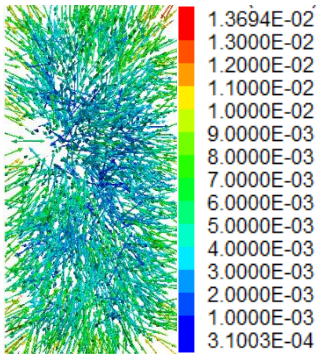

(1) b_e = 20%

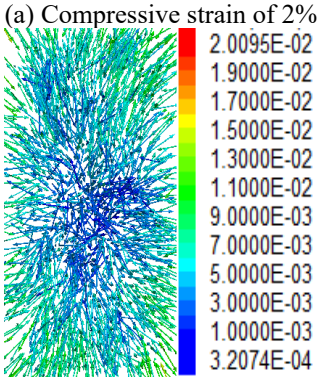

(2) b_e = 40%

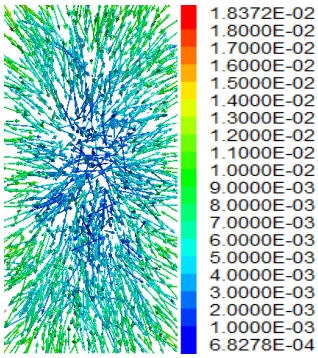

(3) b_e = 60%

(b) Compressive strain of 4%

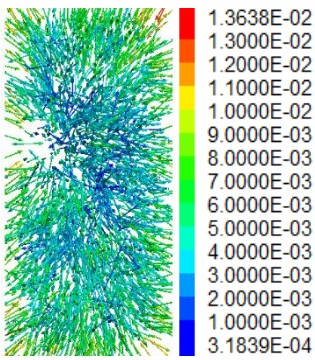

(1) b_e = 20%

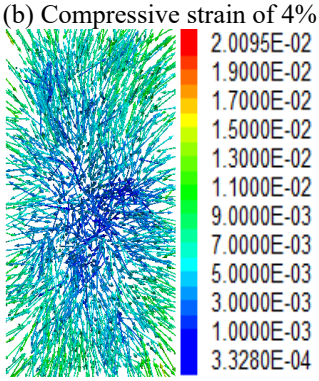

(2) b_e = 40%

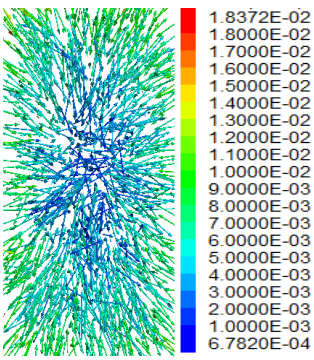

(3) b_e = 60%

(c) Compressive strain of 5%

Fig. 9 Change law of displacement field of lightweight soil with different EPS particle volume ratios (σ_3 = 100 kPa, σ_d = 180 kPa, unit of displacement: m)

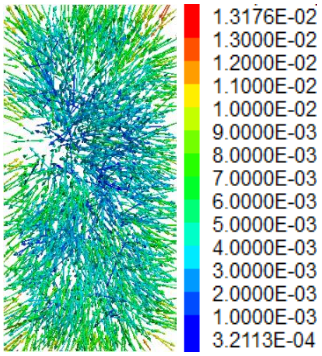

(1) b_e = 20%

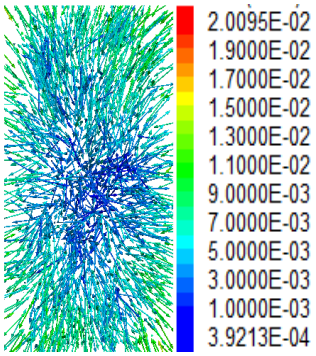

(2) b_e = 40%

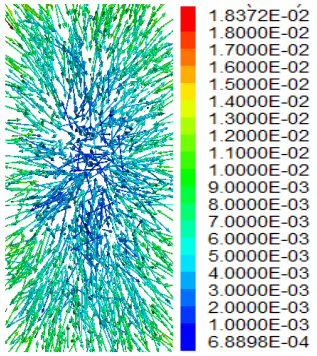

(3) b_e = 60%

(d) Compressive strain of 8%

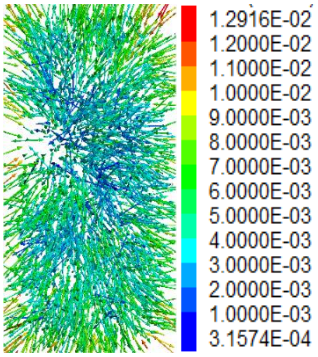

(1) b_e = 20%

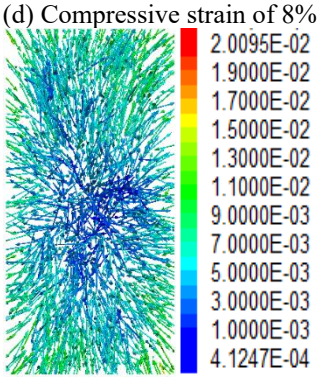

(2) b_e = 40%

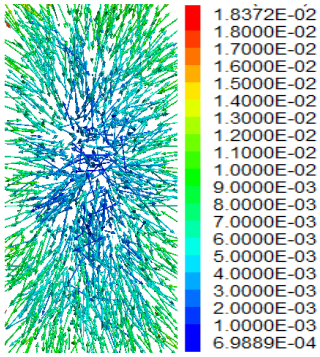

(3) b_e = 60%

(e) Compressive strain of 10%

Fig. 9 Continued-

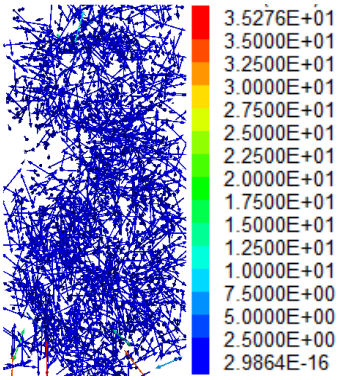

(1) b_e = 20%

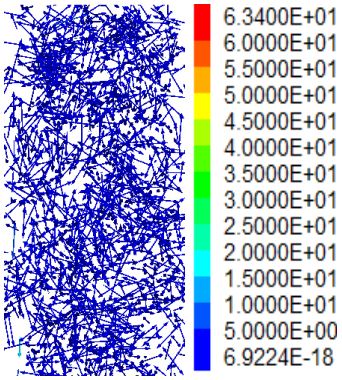

(2) b_e = 40%

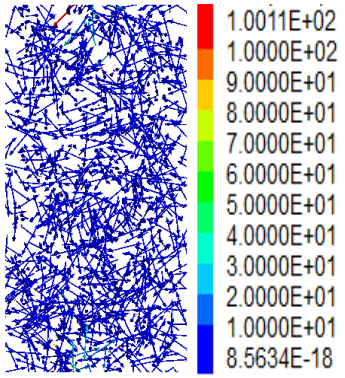

(3) b_e = 60%

(a) Compressive strain of 2%

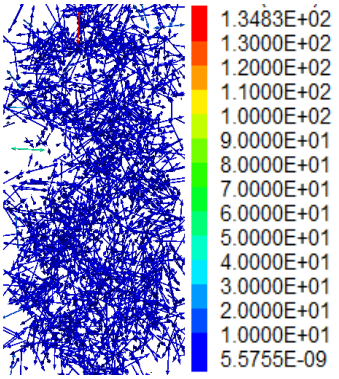

(1) b_e = 20%

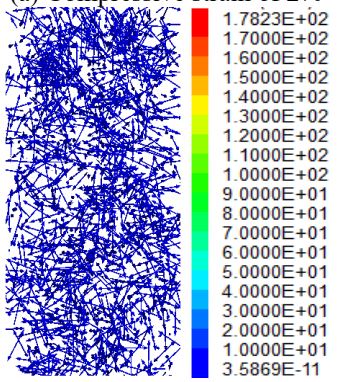

(2) b_e = 40%

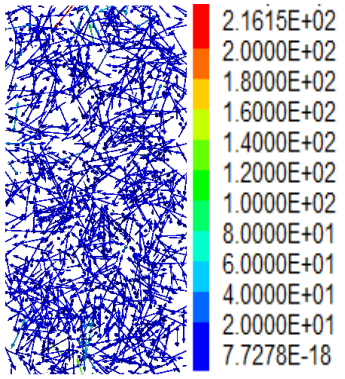

(3) b_e = 60%

(b) Compressive strain of 4%

Fig. 10 Change law of velocity field of lightweight soil with different EPS particle volume ratios (σ_3 = 100 kPa, σ_d = 180 kPa, unit of velocity: m/s

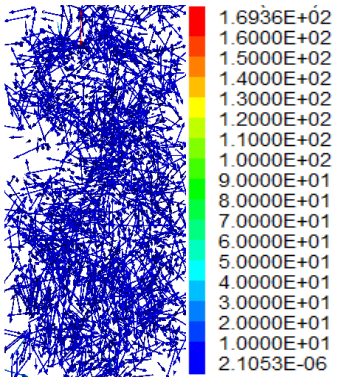

(1) b_e = 20%

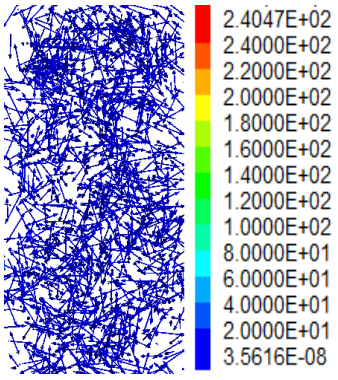

(2) b_e = 40%

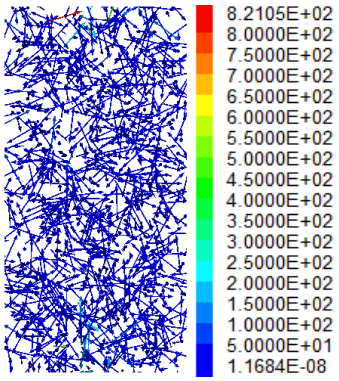

(3) b_e = 60%

(c) Compressive strain of 5%

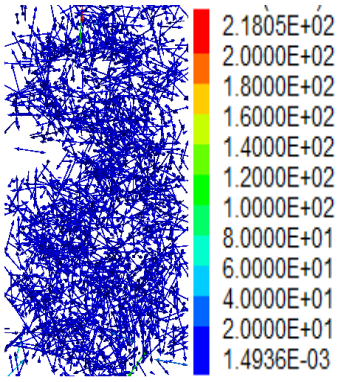

(1) b_e = 20%

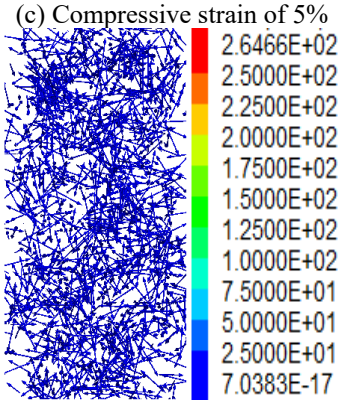

(2) b_e = 40%

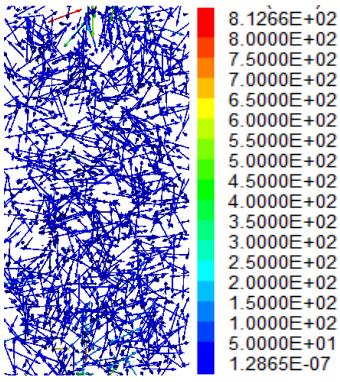

(3) b_e = 60%

(d) Compressive strain of 8%

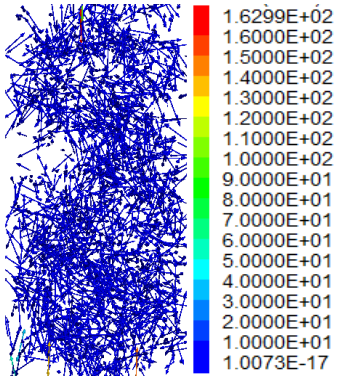

(1) b_e = 20%

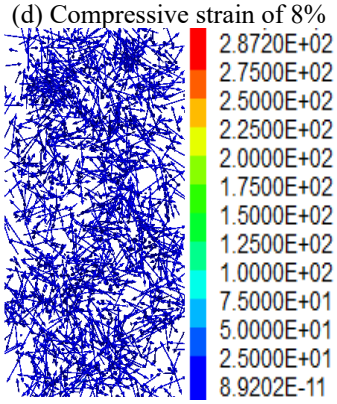

(2) b_e = 40%

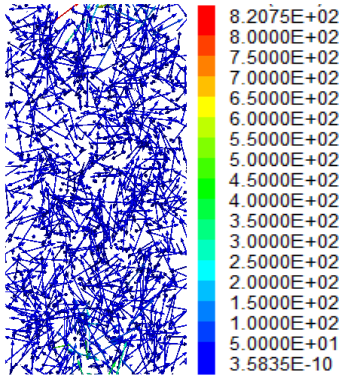

(3) b_e = 60%

(e) Compressive strain of 10%

Fig. 10 Continued-

not possible. In civil engineering, a certain degree of plastic failure is generally allowed, but brittle failure is not allowed. Therefore, in actual engineering applications, the EPS particle volume ratio cannot be extremely large or small. The EPS particle volume ratio should be determined to satisfy the requirements of strength and stability. At 5% strain, the contact force of the particles changed significantly and the number of particles deflected in the velocity direction increased considerably; this is consistent with the trend in which the test hysteresis curves began to change from dense to sparse at 5% strain. These results indicated that the structure of the lightweight soil was destroyed at this time, and 5% compressive strain was technically the strength failure standard of the lightweight soil.

Table 5 Dynamic triaxial test numerical simulation scheme of lightweight soil under different amplitudes

Mixed ratio	Confining pressure /σ_3 (kPa)	Amplitude /σ_d (kPa)
a_c = 15%, b_e = 60%	100	55, 70, 85, 100

4.2 Effect of amplitude on microscopic mechanical characteristics of lightweight soil

Samples with a cement content of 15% and an EPS particle volume ratio of 60% were loaded at different amplitudes. In the simulation process, the loading was stopped when the compressive strain reached the set value for the first time. The test scheme is presented in Table 5.

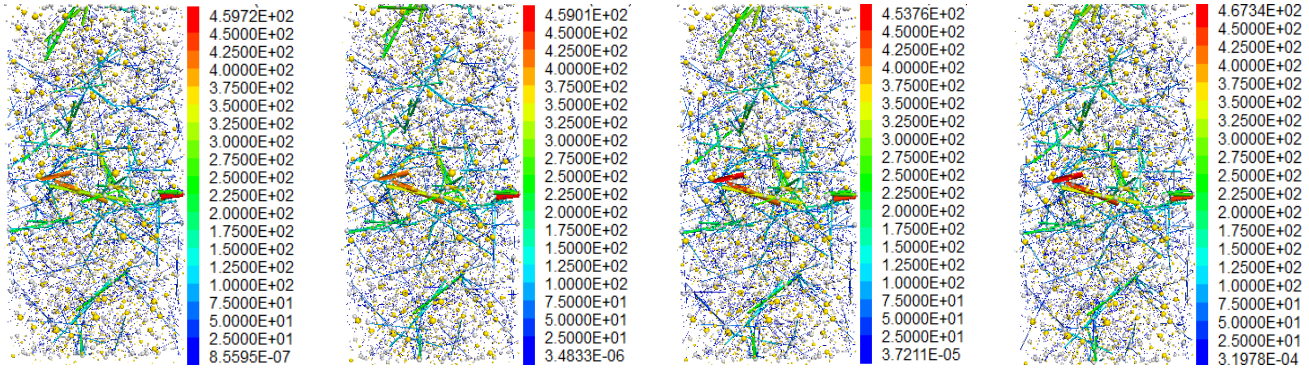

(1) Amplitude 55 kPa (2) Amplitude 70 kPa (3) Amplitude 85 kPa (4) Amplitude 100 kPa

(a) Compressive strain of 2%

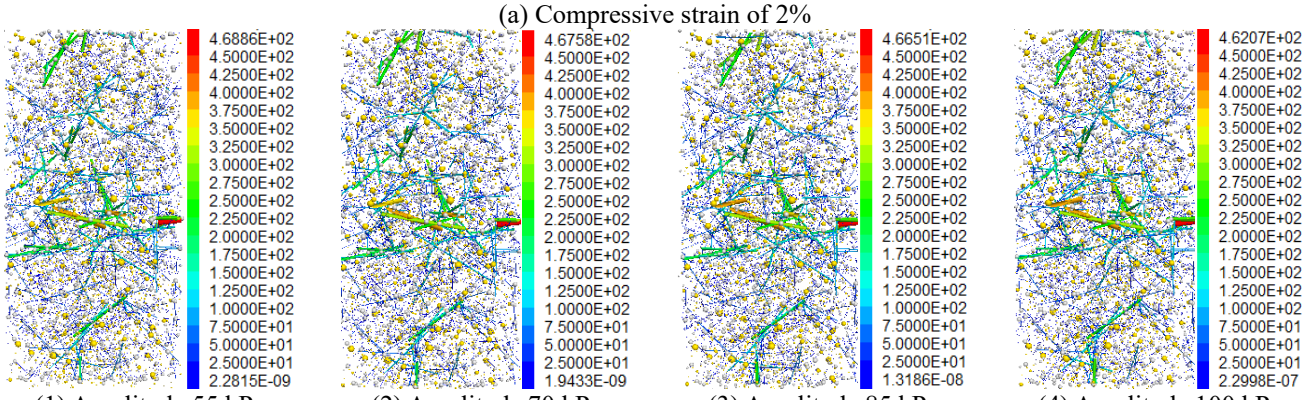

(1) Amplitude 55 kPa (2) Amplitude 70 kPa (3) Amplitude 85 kPa (4) Amplitude 100 kPa

(b) Compressive strain of 4%

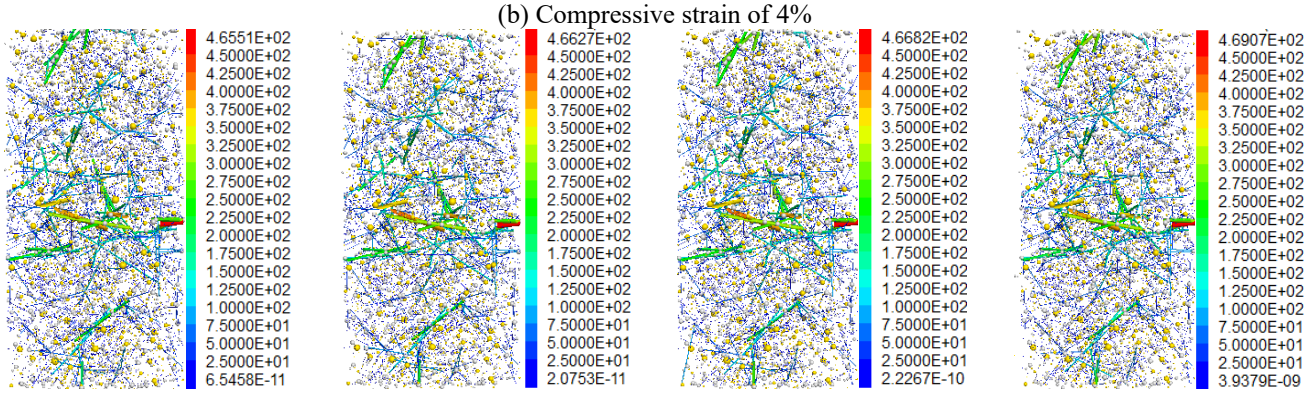

(1) Amplitude 55 kPa (2) Amplitude 70 kPa (3) Amplitude 85 kPa (4) Amplitude 100 kPa

(c) Compressive strain of 5%

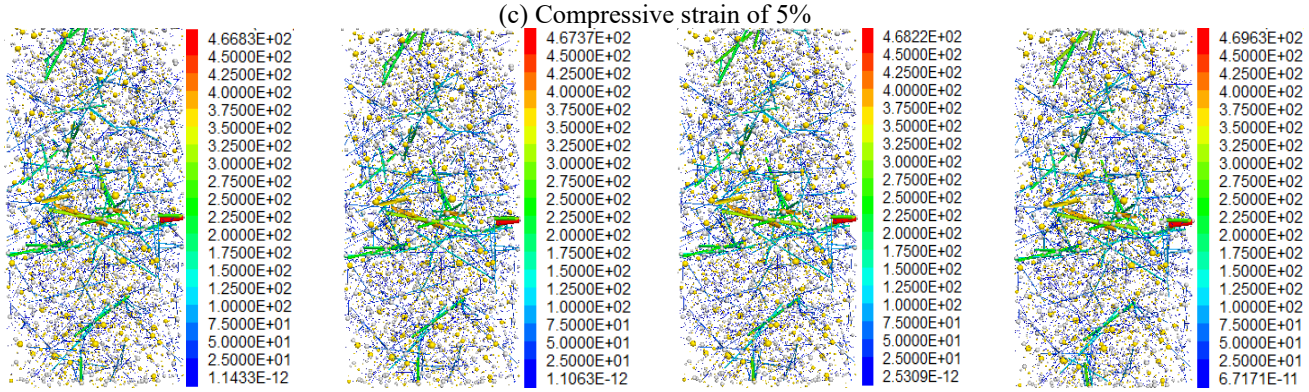

(1) Amplitude 55 kPa (2) Amplitude 70 kPa (3) Amplitude 85 kPa (4) Amplitude 100 kPa

(d) Compressive strain of 8%

Fig. 11 Change law of contact force of lightweight soil under different amplitudes (a_c = 15%, b_e = 40%, σ_3 = 100 kPa, unit of contact force: N)

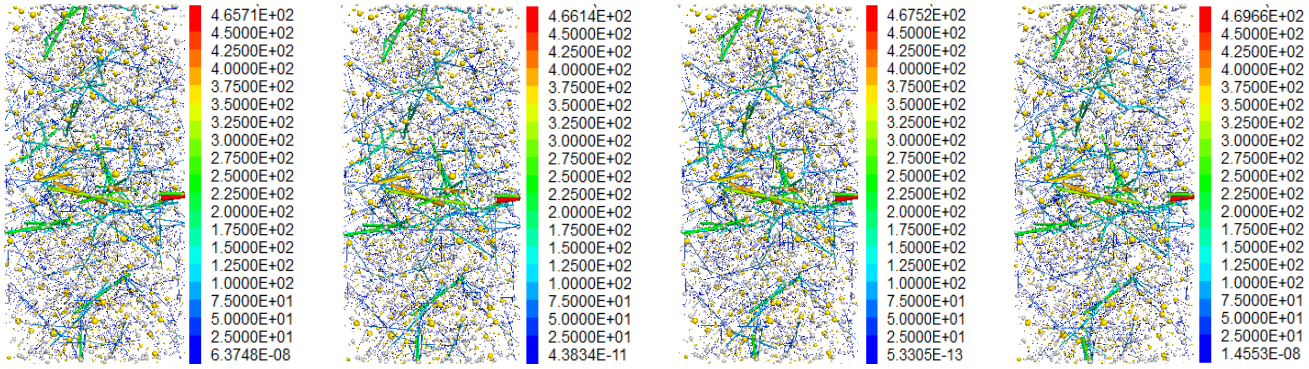

(1) Amplitude 55 kPa (2) Amplitude 70 kPa (3) Amplitude 85 kPa (4) Amplitude 100 kPa

(e) Compressive strain of 10%

Fig. 11 Continued-

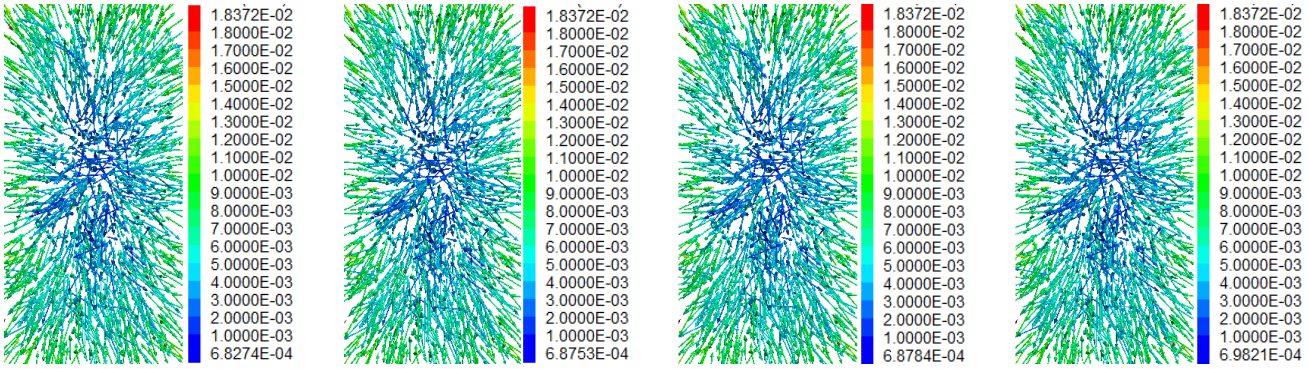

(1) Amplitude 55 kPa (2) Amplitude 70 kPa (3) Amplitude 85 kPa (4) Amplitude 100 kPa

(a) Compressive strain of 2%

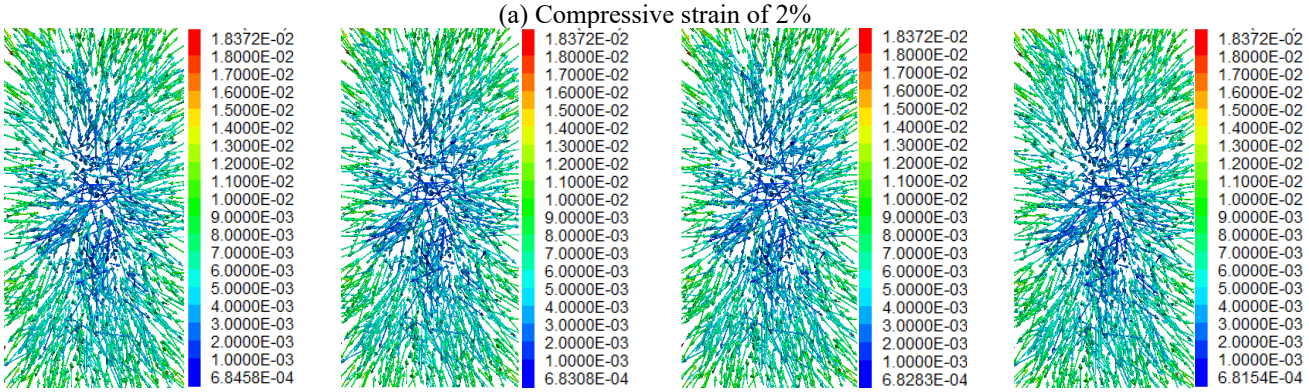

(1) Amplitude 55 kPa (2) Amplitude 70 kPa (3) Amplitude 85 kPa (4) Amplitude 100 kPa

(b) Compressive strain of 4%

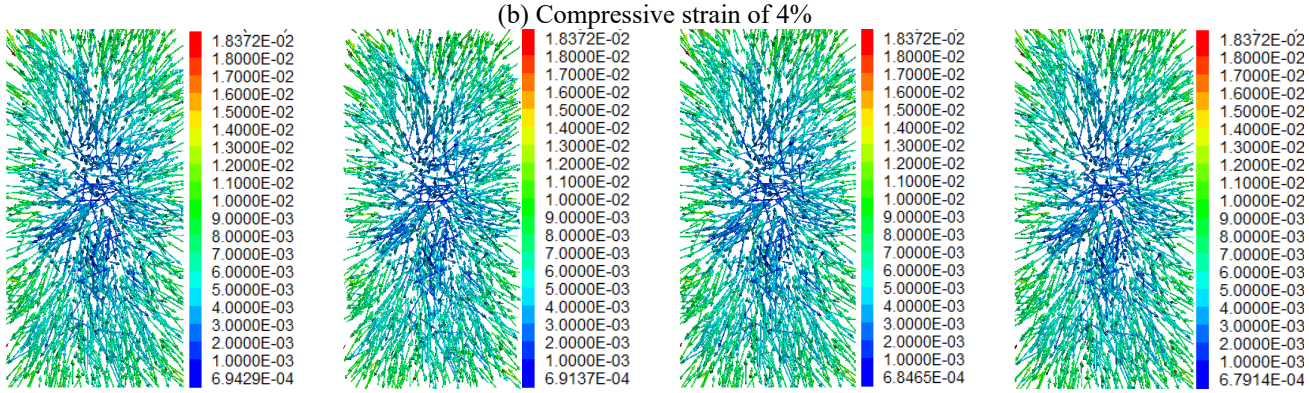

(1) Amplitude 55 kPa (2) Amplitude 70 kPa (3) Amplitude 85 kPa (4) Amplitude 100 kPa

(c) Compressive strain of 5%

Fig. 12 Change law of displacement field of lightweight soil under different amplitudes (a_c = 15%, b_e = 40%, σ_3 = 100 kPa, unit of displacement: m)

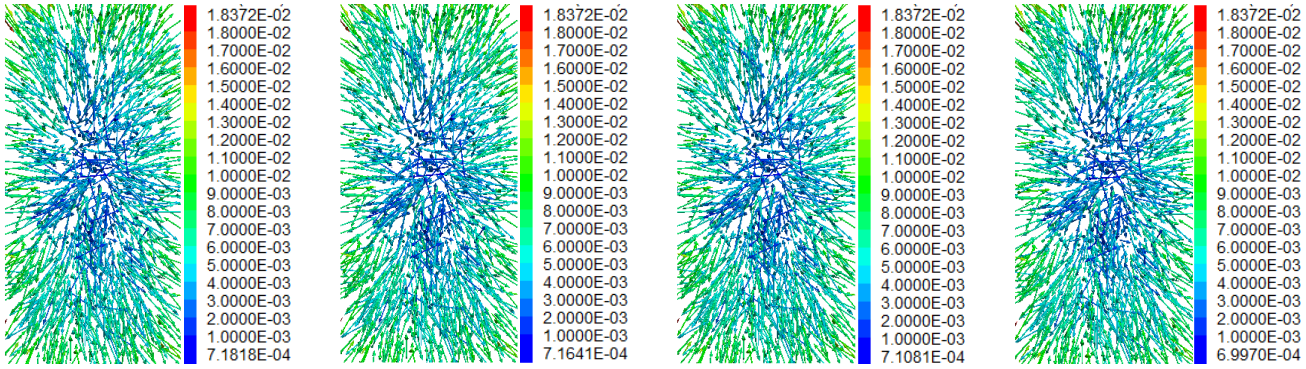

(1) Amplitude 55 kPa (2) Amplitude 70 kPa (3) Amplitude 85 kPa (4) Amplitude 100 kPa

(d) Compressive strain of 8%

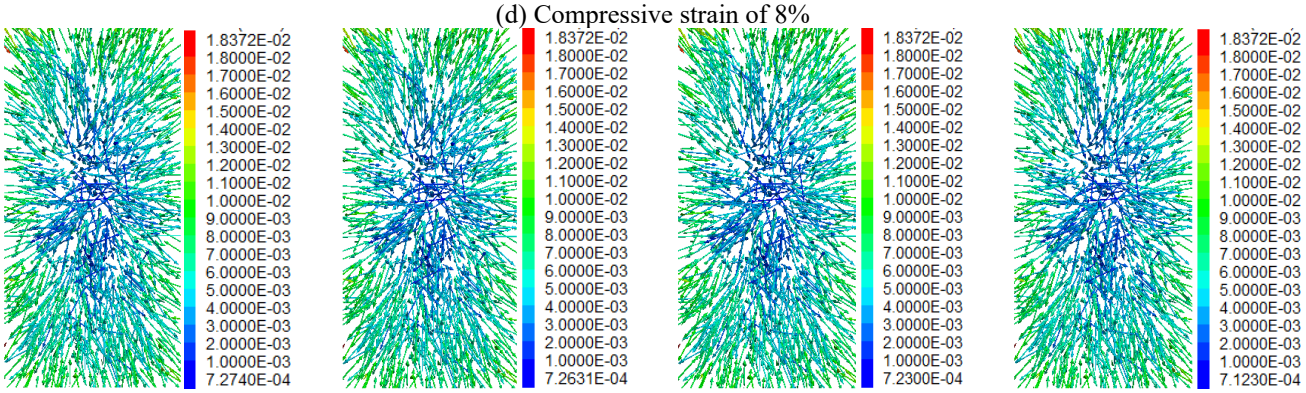

(1) Amplitude 55 kPa (2) Amplitude 70 kPa (3) Amplitude 85 kPa (4) Amplitude 100 kPa

(e) Compressive strain of 10%

Fig. 12 Continued-

(1) Contact forces

Fig. 11 displays the following: (1) the maximum contact force increases with an increase in amplitude. This shows that an increase in amplitude reduces the number of pores between particles and increases the contact force of the particles. (2) The force chain distribution between the soil particles exhibits little change. With an increase in the amplitude, the force chain between the EPS particles changes. The size of the force chain is related to the displacement between the particles. Because the stiffnesses of EPS particles and soil particles are different, the force chain between soil particles is larger. The deformation of the EPS particles is mainly slip and movement in the early stage of vibration, and the soil particles begin to move in the later stage of vibration. The force chain skeleton of lightweight soil is formed by the force chain between soil particles.

(2) Displacement field

Fig. 12 depicts the following: (1) the particle displacement at both ends of the sample is larger, and the particle displacement at the middle is smaller. (2) The particle displacement field is symmetrically distributed along the horizontal cross section in the middle part of the sample. (3) When the confining pressure is constant, the numerical value of the particle displacement changes slightly with the increase in amplitude, whereas the distribution of the displacement field does not change significantly with the increase in compressive strain. (4) The average particle displacement increases with the increase in compressive strain.

The maximum particle displacement is not significantly affected by the amplitude, and the bonding force between the EPS particles is very small. Bonding breaks in the range of small vibration amplitudes. The EPS particle volume ratio in the sample is 60%, and the displacement of the particles is dominated by the EPS particles. In the late vibration period, the bonds between soil particles are gradually destroyed, and the displacement of the soil particles with smaller displacements increases with the vibration.

(3) Velocity field

Fig. 13 presents the following: (1) the velocity of the particles at both ends is greater than that of the particles in the middle. With an increase in the amplitude, the velocity of the particles increases gradually. (2) At the initial stage of vibration, the velocities of the particles at both ends are mainly radial. The velocity direction exists in both the radial direction towards and away from the center of the circle in the cross section of the soil sample. The vertical motion of the central particles is mainly directed towards the center of the sample. With the increase in compressive strain, the direction of particle velocity at both ends gradually turns to the vertical direction pointing to the center of the sample in the longitudinal section of the soil sample. (3) At the same amplitude, the particle velocity increases with the increase in compressive strain.

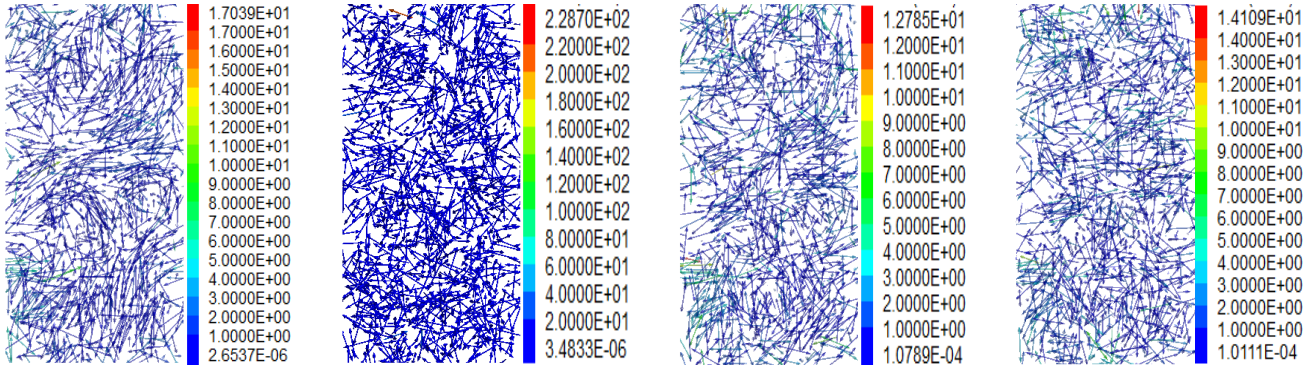

(1) Amplitude 55 kPa (2) Amplitude 70 kPa (3) Amplitude 85 kPa (4) Amplitude 100 kPa

(a) Compressive strain of 2%

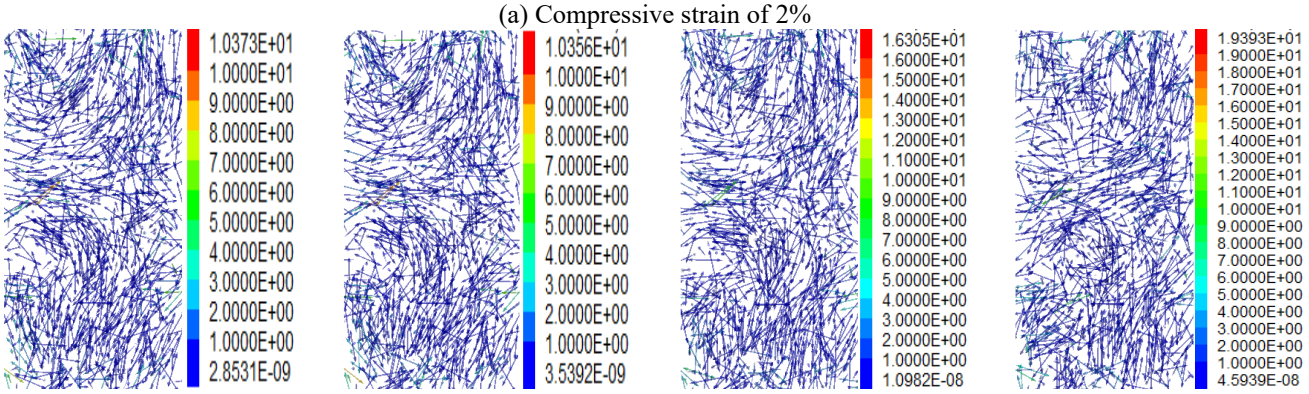

(1) Amplitude 55 kPa (2) Amplitude 70 kPa (3) Amplitude 85 kPa (4) Amplitude 100 kPa

(b) Compressive strain of 4%

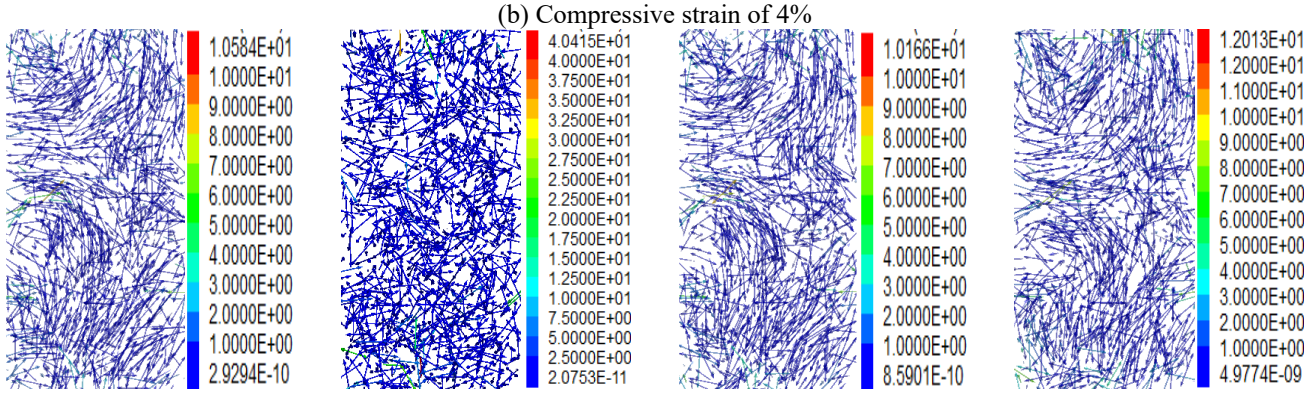

(1) Amplitude 55 kPa (2) Amplitude 70 kPa (3) Amplitude 85 kPa (4) Amplitude 100 kPa

(c) Compressive strain of 5%

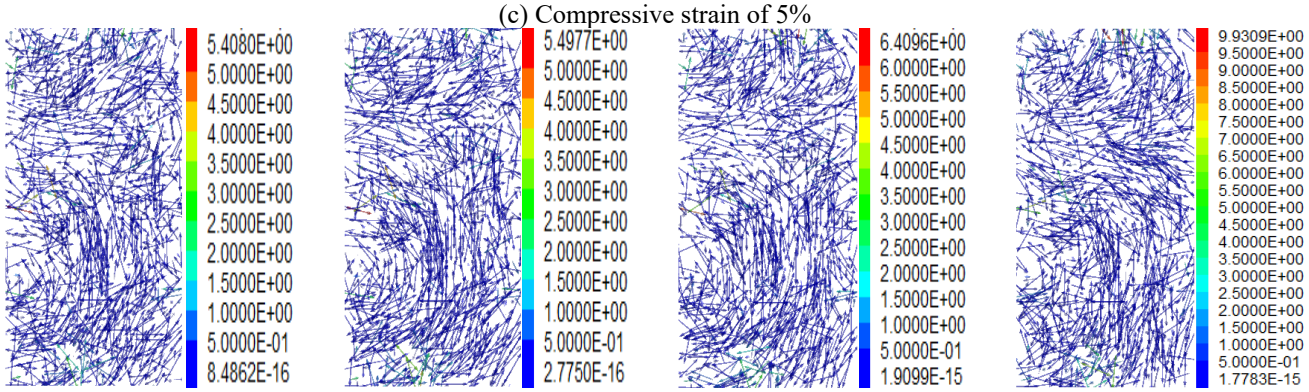

(1) Amplitude 55 kPa (2) Amplitude 70 kPa (3) Amplitude 85 kPa (4) Amplitude 100 kPa

(d) Compressive strain of 8%

Fig. 13 Change law of velocity field of lightweight soil under different amplitudes (a_c = 15%, b_e = 40%, σ_3 = 100 kPa, unit of velocity: m/s)

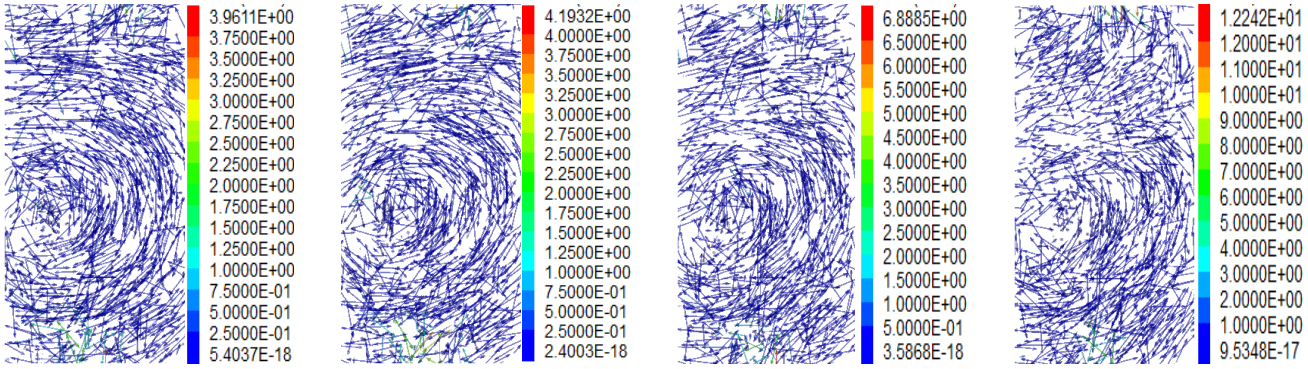

(1) Amplitude 55 kPa (2) Amplitude 70 kPa (3) Amplitude 85 kPa (4) Amplitude 100 kPa

(e) Compressive strain of 10%

Fig. 13 Continued-

Under the condition of constant confining pressure, an increasing amplitude increases the dynamic stress of the particle system, and the dynamic strain accumulation rate of the sample increases. Macroscopically, when the confining pressure is constant, the larger the amplitude, the smaller is the number of the vibration cycles when the same dynamic strain is reached. The vertical movement of the particles in the initial stage indicates that the distance between the samples is small and that the samples are compacted. In the later stage, with an increase in cumulative strain, the samples enter the failure stage, and the velocity value of the internal particles increases. This indicates that the bond between the samples is destroyed, and the soil loses its original strength.

Cyclic loading on soil has two mechanical effects: cyclic and rate effects. The cyclic effect appears as the vibration time in the harmonic load, and the rate effect is related to the load frequency and amplitude. When the frequency is constant, different amplitudes exhibit different rate effects. With the increase in the amplitude, the maximum acceleration of the load increases, causing bond fracture of the particle system and displacement of the particles at an earlier time. For lightweight soil samples, because the bond among EPS particles is the weakest, the contact force chain among EPS particles breaks during the early stage of vibration. With an increase in the vibration time, the contact force chain between the soil particles breaks. The figures for the contact force show that the soil particles are more distributed in the middle of the sample than far away from the center. With an increase in compressive strain, the movement of particles at both ends of the sample drives the middle particles. The transmission of the force chain is lagging, resulting in the change in the particle velocity direction in the middle of the sample lagging behind the particles at both ends of the sample. The greater the amplitude, the greater is the maximum acceleration value of the load and earlier the change in particle velocity direction occurs.

5. Conclusions

• The hysteresis curves of remolded soil and lightweight soil exhibited the characteristics of nonlinearity, hysteresis, and strain accumulation. The strain accumulated in remolded soil was mainly tensile strain, and that in lightweight soil was mainly compressive strain. With an increase in the vibration frequency, the hysteresis curves of the remolded soil and lightweight soil changed from dense to sparse. The amplitudes of the tension and compression half-cycles of the hysteresis curves for lightweight soils were not equal. The amplitude of the tension half-cycle was less than that of the compression half-cycle. The amplitudes of the tension and compression half-cycles of the hysteresis curves for the remolded soil were equal.

• With an increase in the EPS particle volume ratio, the contact force increased initially and then decreased, and the particle displacement and velocity increased. An increase in the EPS particle volume ratio indicated a decrease in the number of soil particles in the sample. For lightweight soil samples, the strength of the bond between soil particles was the basis of the strength of the lightweight soil. The larger the EPS particle volume ratio, the lower the strength of the soil, the smaller the constraint between particles, and the more the soil was to fracture failure of the bond. Under the same dynamic stress, the velocity and displacement values of the particles were larger.

• The maximum value of the contact force increased with increase in the amplitude. The maximum displacement of the particles was not significantly affected by the amplitude. The bond between the EPS particles was very small, and the bond broke in the low range of vibration amplitudes. The larger the amplitude, the earlier was the deflection of the particle velocity direction. The increase in amplitude increased the dynamic stress effect on the particle system and the dynamic strain accumulation rate of the sample.

• At 5% strain, the contact force of the particles changed significantly and the number of particles deflecting in the direction of velocity increased substantially. This was consistent with the trend of the test hysteresis curves beginning to change from dense to sparse at 5% strain. These results showed that the damage to the structure of the lightweight soil began at this time. Thus, 5% compressive strain can be reasonably considered as the dynamic strength failure criterion for lightweight soil.

Acknowledgments

Project (51509211) supported by the National Natural Science Foundation of China; Project (2016M602863) supported by China Postdoctoral Science Foundation; Project (2018031) supported by the Excellent Science and Technology Activities Foundation for Returned Overseas Teachers of Shaanxi Province; Project (2015SF260) supported by the Social Development Foundation of Shaanxi Province; Project (2017BSHYDZZ50) supported by the Postdoctoral Science Foundation of Shaanxi Province; Project (2021JLM-51) supported by the Natural Science Foundation of Shaanxi Province; Project (SZ02306) supported by Shaanxi Key Laboratory of Safety and Durability of Concrete Structures, Xijing University; Project (XKLGUEKF21-02) supported by Xi'an Key Laboratory of Geotechnical and Underground Engineering, Xi'an University of Science and Technology; Project (2452020169) supported by the Fundamental Research Funds for the Central Universities.

References

Anandarajah, A. (1994), "Discrete-element method for simulating behavior of cohesive soil", *J. Geotech. Eng.*, **9**(120), 1593-1613. https://doi.org/10.1016/0148-9062(95)99122-E.

Batiste, S., Alshibli, K., Sture, S. and Lankton, M. (2004), "Shear band characterization of triaxial sand specimens using computed tomography", *Geotech. Test. J.*, **27**(6), 568-579. https://doi.org/10.1520/GTJ12080.

Bono, D., Mcdowell, G.R. and Wanatowski, D. (2012), "Discrete element modelling of a flexible membrane for triaxial testing of granular material at high pressures", *Géotechnique Lett.*, **2**(4), 199-203. https://doi.org/10.1680/geolett.12.00040.

Cundall, P.A. and Strack, O.D.L. (1979), "A discrete numerical model for granular assemblies", *Géotechnique*, **29**(1), 47-65. https://doi.org/10.1680/geot.1979.29.1.47.

Dong, L., Hou, T.S. and Luo, Y.S. (2019), "Dynamic strength parameters of light wright soil mixed with EPS beads", *J. Northwest A&F University (Natural Science Edition)*, **47**(5), 139-145. https://doi.org/10.13207/j.cnki.jnwafu.2019.05.018.

Dong, Y. and Fatahi, B. (2020), "Discrete element simulation of cavity expansion in lightly cemented sands considering cementation degradation", *Comput. Geotech.*, **124**, https://doi.org/10.1016/j.compgeo.2020.103628.

GB/T50123 (2019), Standard for Soil Test Method, Ministry of Water Resources of People's Republic of China; Beijing, China.

Hou, T.S. (2021), "Influence law of characteristic water content on basic properties of light weight soil", *Rock Soil Mech.*, **33**(9), 2581-2587. https://doi.org/10.16285/j.rsm.2012.09.004.

Hou, T.S. and Xu, G.L. (2009), "Experiment on triaxial pore water pressure-stress-strain characteristics of foamed particle light weight soil", *China J. Highway Transport*, **22**(6), 10-17. https://doi.org/10.19721/j.cnki.1001-7372.2009.06.002.

Hou, T.S. and Xu, G.L. (2010), "Experimental study on the shear strength characteristics of foamed particle light weight soil", *J. China Univ. Min Tech.*, **39**(4), 534-540. http://www.cnki.com.cn/Article/CJFDTotalZGKD201004011.htm.

Hou, T.S. and Xu, G.L. (2011), "Influence law of EPS size on shear strength of light weight soil", *Chinese J. Geotech. Eng.*, **33**(10), 435-442. http://www.cnki.com.cn/Article/CJFDTotal-YTGC202006026.htm.

Hou, T.S., Xu, G.L. and Lou, J.D. (2011), "Triaxial compression test on shear strength characteristics of light weight sand", *J. Central South Univ. (Science and Technology)*, **42**(11), 3521-3529. https://doi.org/10.3969/j.issn.1000-7598.2011.10.016.

Jin, L., Zeng, Y.W., Xia, L. and Ye, Y. (2017), "Experimental and numerical investigation of mechanical behaviors of cemented soil–rock mixture", *Geotech. Geol. Eng.*, **35**(1), 337-354. https://doi.org/10.1007/s10706-016-0109-4.

Lan, X., Hou, T.S., Yang, Y. and Zhang, Y.F. (2020), "Discrete element analysis on dynamic deformation characteristics of light weight soil mixed with EPS particles", *J. Civil Eng. Management*, **37**(3), 147-154. https://doi.org/10.3969/j.issn.2095-0985.2020.03.024.

Li, T., Jiang, M.J. and Sun, R.H. (2020), "DEM analysis of evolution law of bond degradation for structured soils", **42**(6), 1159-1166. https://d.wanfangdata.com.cn/periodical/ytgcxb202006023.

Lv, X.L., Zeng, S., Li, L.C., Qian, J.G. and Huang, M.S. (2019), "Two-dimensional discrete element simulation of the mechanical behavior and strain localization of anisotropic dense sands", *Granular Matter*, **21**(2), 1-16. https://doi.org/10.1007/s10035-019-0891-9.

Wang, Y.H. and Leung, S.C. (2008), "Characterization of cemented sand by experimental and numerical investigations", *J. Geotech. Geoenviron. Eng.*, **134**(7), 992-1004. https://doi.org/10.1061/(ASCE)1090-0241(2008)134:7(992).

Wu, S.C. and Xu, X. (2016), "A study of three intrinsic problems of the classic discrete element method using flat-joint model", *Rock Mech. Rock Eng.*, **49**(5), 1813-1830. https://doi.org/10.1007/s00603-015-0890-z.

Xu, W.J., Hu, L.M. and Gao, W. (2016), "Random generation of the meso-structure of a soil-rock mixture and its application in the study of the mechanical behavior in a landslide dam", *Int. J. Rock Mech. Min. Sci.*, **86**, 166-178. https://doi.org/10.1016/j.ijrmms.2016.04.007.

Yang, Z.P., Tian, X., Lei, X.D., Jiang, Y.W., Liu, X.R. and Hu, Y.X. (2020), "Particle discrete element numerical study on factors of shear strength characteristics for soil-rock mixture", *Eng. Geol.*, **28**(1), 39-50. https://doi.org/10.13544/j.cnki.jeg.2019-285.

Zhang, F.G., Nie, Z.C., Chen, M.F. and Feng, H.P. (2021), "DEM analysis of macro- and micro-mechanical behaviors of cemented sand subjected to undrained cyclic loading", *Chinese J. Geotech. Eng.*, **43**(3), 456-464. http://manu31.magtech.com.cn/Jwk_ytgcxb/CN/10.11779/CJGE202103008.

Zhou, Y.D., He, Q.B., Feng, T.G. and Lu, R. (2008), "Comparative researches on dynamic strength properties of lightweight clay-EPS beads soil", *J. Hohai Univ. (Natural Sciences)*, **36**(6), 810-813. https://doi.org/10.3876/j.issn.1000-1980.2008.06.018.

GC